Cardiovasc Intervent Radiol (2022) 45:306–314
https://doi.org/10.1007/s00270-021-03035-5

SCIENTIFIC PAPER (OTHER) INTERVENTIONAL ONCOLOGY

In Vivo Comparison of Micro-Balloon Interventions (MBI) Advantage: A Retrospective Cohort Study of DEB-TACE Versus b-TACE and of SIRT Versus b-SIRT

Pierleone Lucatelli[1] · Gianluca De Rubeis[1,2] · Claudio Trobiani[1] · Sara Ungania[3] · Bianca Rocco[1] · Simone Zilahi De Gyurgyokai[1] · Marica Masi[3] · Irene Pecorella[4] · Federico Cappelli[5] · Quirino Lai[6] · Carlo Catalano[4] · Giulio Vallati[5]

Received: 9 June 2021 / Accepted: 25 November 2021 / Published online: 17 January 2022

Abstract

Purpose The purpose of this study was to evaluate in vivo the role of the micro-balloon by comparing trans-arterial chemoembolization (DEB-TACE) and selective internal radiotherapy (SIRT) procedures performed with and without balloon micro-catheter (b-DEB-TACE and DEB-TACE/SIRT and b-SIRT) for the treatment of hepatocellular carcinoma (HCC).

Methods The impact of a balloon micro-catheter on trans-arterial loco-regional treatment was analyzed using non-enhanced post-procedural cone-beam CT (Ne-CBCT) by comparing the attenuation values in the embolized area and the surrounding liver tissue before and after DEB-TACE versus b-DEB-TACE and by comparing 2D/3D dosimetry in single-photon emission computed tomography after SIRT versus b-SIRT, and by comparing the histological count of the beads following orthotopic liver transplantation in the DEB-TACE versus b-DEB-TACE subgroup.

Results We treated 84 HCC patients using trans-arterial loco-regional therapy. Fifty-three patients (26 DEB-TACE and 27 b-DEB-TACE) were analyzed in the TACE group. Contrast, signal-to-noise ratio, and contrast-to-noise ratio were all significantly higher in b-DEB-TACE subgroup than DEB-TACE (182.33 HU [CI95% 160.3–273.5] vs. 124 HU [CI95% 80.6–163.6]; 8.3 [CI95% 5.7–10.1] vs. 4.5 [CI95% 3.7–6.0]; 6.9 [CI95% 4.3–7.8] vs. 3.1 [CI95%

✉ Pierleone Lucatelli
pierleone.lucatelli@gmail.com

Gianluca De Rubeis
derubeis.gianluca@gmail.com

Claudio Trobiani
claudio.trobiani@gmail.com

Sara Ungania
sara.ungania@gmail.com

Bianca Rocco
biancarocco.br@gmail.com

Simone Zilahi De Gyurgyokai
simonezilahi@hotmail.it

Marica Masi
marica.masi1991@gmail.com

Irene Pecorella
irene.pecorella@uniroma1.it

Federico Cappelli
federicocappelli@hotmail.it

Quirino Lai
lai.quirino@libero.it

Carlo Catalano
carlo.catalano@uniroma1.it

Giulio Vallati
giulio.vallati@ifo.gov.it

[1] Vascular and Interventional Radiology Unit, Department of Diagnostic Service, Sapienza University of Rome, Viale Regina Elena 324, 00161 Rome, Italy

[2] Department of Diagnostic Radiology, Azienda Ospedaliera San Camillo Forlanini, Rome, Italy

[3] Physics Department of "Istituto Regina Elena Istituto di Ricovero e Cura a Carattere Scientifico", Rome, Italy

[4] Department of Radiological Sciences, Oncology and Anatomical Pathology, Policlinico Umberto I, University of Rome "Sapienza", Rome, Italy

[5] Interventional Radiology Unit of "Istituto Regina Elena Istituto di Ricovero e Cura a Carattere Scientifico", Rome, Italy

[6] Department of General Surgery and Organ Transplantation, Sapienza University of Rome, Rome, Italy

2.2–5.0] $p < 0.05$). Thirty-one patients (24 SIRT and 7 b-SIRT) were analyzed in the SIRT group. 2D dosimetry profile evaluation showed an activity intensity peak significantly higher in the b-SIRT than in the SIRT subgroup (987.5 ± 393.8 vs. 567.7 ± 302.2, $p = 0.005$). Regarding 3D dose analysis, the mean dose administered to the treated lesions was significantly higher in the b-SIRT than in the SIRT group (151.6 Gy ± 53.2 vs. 100.1 Gy ± 43.4, $p = 0.01$). In histological explanted liver analysis, there was a trend for higher intra-tumoral localization of embolic microspheres for b-DEB-TACE in comparison with DEB-TACE.

Conclusions Due to the use of three different methods, the results of this study demonstrate in vivo, a better embolization profile of oncological intra-arterial interventions performed with balloon micro-catheter regardless of the embolic agent employed.

Keywords SIRT · b-SIRT · DEB-TACE · b-DEB-TACE · SPECT

Abbreviations

b-DEB-TACE	Balloon occluded trans-arterial chemoembolization
B-SIRT	Balloon occluded selective internal radiotherapy
CT	Computed tomography
DEB-TACE	Drug-eluting beads trans-arterial chemoembolization
HCC	Hepatocellular carcinoma
MBI	Micro-balloon interventions
Ne-CBCT	Non enhanced cone-beam CT
OLT	Orthotopic liver transplantation
PEG	Polyethylene glycol
SIRT	Selective internal radiotherapy
SPECT	Single-photon emission computed tomography
TACE	Trans-arterial chemoembolization

Introduction

Micro-balloon interventions (MBI) have gained popularity in the field of liver embolization procedures introducing a new concept, namely the possibility to perform a pressure gradient-driven embolization. To date, scientific efforts have been pursued to understand the safety profile and the oncological response of balloon occluded trans-arterial chemoembolization (b-TACE) procedures with all the different embolic agents (Lipiodol c-TACE, drug-eluting beads DEB-TACE) [1–4], and balloon occluded selective internal radiotherapy (b-SIRT) [3]. Despite this, in vivo comparison of the ability of the micro-balloon catheter to ameliorate embolic agent distribution within the target lesion remains scarce.

Several in-vivo methodologies may be used to quantify the efficacy of catheter-based treatment. Non-enhanced Cone-Beam CT (Ne-CBCT) can display drug and beads deposition because these are mixed with contrast media during trans-arterial chemoembolization (TACE) procedures. Moreover, due to its tri-dimensional nature, Ne-CBCT can perform a pseudo-attenuation measurement by manually segmenting all the target nodules as well as the surrounding liver parenchyma and by recording both signal (as pseudo-HU) and noise (as standard deviation, SD) [5]. Ne-CBCT is technically similar to computed tomography (CT) but does not allow to perform HU measurements, therefore pseudo-attenuation is the measurable parameter in Ne-CBCT.

SPECT/CT permits personalized dosimetry to accurately assess post-SIRT activity distribution and effectively absorbed dose calculation (expressed in Gray, Gy) using dedicated software. Finally, specimen analysis of explanted liver after orthotopic liver transplantation (OLT) can permit direct count and localization of beads on the targeted treatment area [6, 7]. Thus, the rationale for employing these three different independent methods is the possibility of using them as observational tools to investigate and quantify the effect of micro-balloon use in determining higher embolic agent deposition within the target lesion.

This retrospective cohort study aims to quantify in vivo the micro-balloon role in two different catheter-based treatments (i.e., TACE and SIRT) performed with and without micro-balloon occlusion for the treatment of naïve HCC patients. The two different treatment modalities were performed during the same period of enrolment in two different institutions with independent hospital clinical practice.

Material and Methods

The ethical institutional review boards of the two centres approved the study. Informed consent for the procedure and anonymized publication of this series of patients was obtained from all participants included in the study.

The decision whether to use a balloon micro-catheter or not was at the discretion of the operator's choice. (Fig. 1, flowchart).

The present study is a cohort retrospective study on the treatment of naïve HCC patients in which intra-group (b-DEB-TACE vs. TACE; b-SIRT vs. SIRT) analysis was conducted without inter-group comparison. The two separate cohort compositions reflect independent hospital clinical practices.

The impact of balloon micro-catheter on trans-arterial loco-regional treatment was analyzed using three methods. In particular, the effect of micro-catheter was evaluated using (1) post-procedural Ne-CBCT (all parameters are summarized in Table 1), (2) histological count of beads following OLT in the subgroup of TACE/b-TACE [5, 9]; and (3) 2D and 3D dosimetry in SPECT after SIRT/b-SIRT [10, 11].

All HCCs were diagnosed with standard radiological criteria for cirrhotic liver [12–14]. HCC arterial enhancement was evaluated through the arterial enhancement ratio. All nodules were manually segmented in circular ROIs and compared with those ones of the adjacent parenchyma (performed three times in different sites and averaged with the exclusion of visible vasculature, bile ducts, and artifacts). The arterial enhancement ratio was calculated by the mean attenuation of the tumor divided by the attenuation of the adjacent normal liver in the arterial phase as derived from Park et al. [8].

The procedures were decided upon a multidisciplinary board of each centre composed of a transplant surgeon, an interventional radiologist, a body radiologist, and a hepatologist. Indication and contraindication for both cohorts followed the international BCLC guidelines.

DEB-TACE and b-DEB-TACE Protocol and Measured Parameters

All procedures were performed by two experienced Interventional Radiologists (> 10 years of clinical practice). The TACE embolization protocol was standardized for both procedures, starting with 100 ± 25 μm followed by 200 ± 50 μm PEG microspheres (LifePearl, Terumo Europe NV, Leuven—Belgium) [6]. The differences between DEB-TACE and b-DEB-TACE included the micro-catheter type, respectively a 2,7 Fr micro-catheter (Progreat, Terumo Europe NV, Leuven—Belgium) or a balloon micro-catheter (Occlusafe, Terumo Europe NV, Leuven—Belgium), and embolization endpoints. For DEB-TACE, the procedure was performed with the catheter as close as possible to the tumor. For b-DEB-TACE procedures, the catheter was positioned proximal to all lesion feeders to maximize the advantage of the balloon. [15]

Microspheres were loaded with 50 mg of doxorubicin each syringe consisting of 2 mL of embolic material (microspheres 100 μm ± 25 or 200 μm ± 50) diluted with contrast media (350 mmol/mL) to reach 20 mL. The embolization protocol was sequential, starting with the smaller microspheres, immediately followed by a second embolization with the larger ones.

The embolization endpoints were ten heartbeats flow stasis for DEB-TACE while for the MBI a composite endpoint was utilized (reflux of microspheres despite

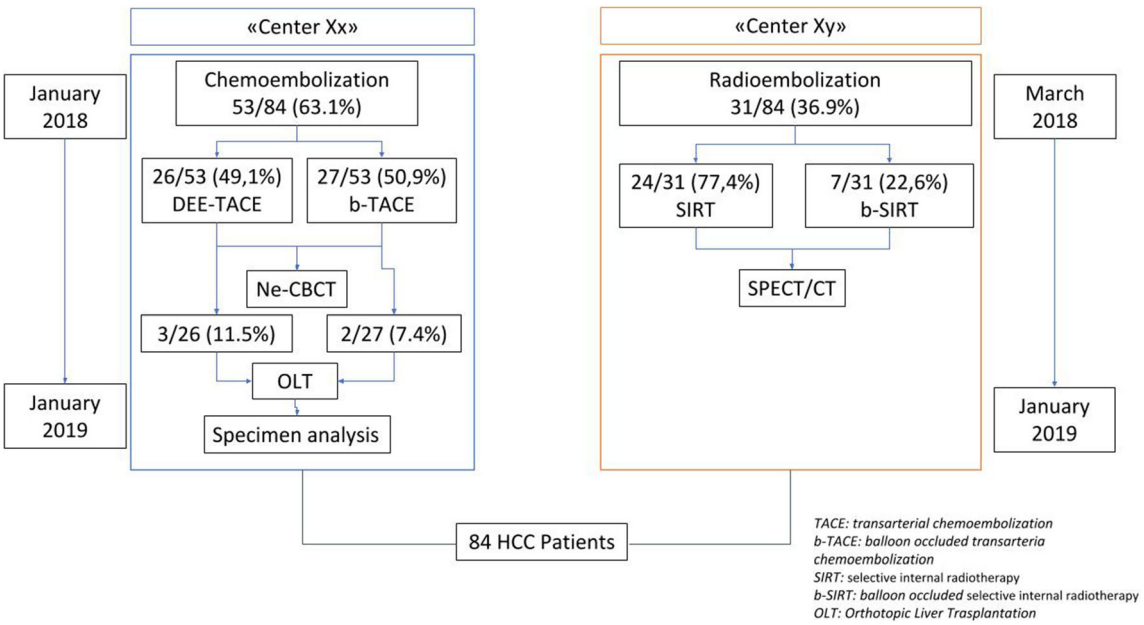

Fig. 1 Study flow-chart

Table 1 Radiological tumoral characteristics of all the patients enrolled

Patients (n = 84)	TACE n = 53 (63.1%)		p	SIRT n = 31 (36.9%)		p
Typology of treatment	B-DEB-TACE	DEB-TACE		B-SIRT	SIRT	
Patients	27/53 (50.9%)	26/53 (49.1%)		7/31 (22.6%)	24/31 (77.4%)	
Median number of nodules treated per patient	1 [CI 95%: 1–2]	1 [CI 95%: 1–1.45]		3.5 [CI: 1–9.2]	4 [CI: 3–5.65]	
Median nodule diameter (mm)	27 [CI 95%: 23.0–35.1]	15.5 [CI 95%: 14–22.5]	0.005	42 [CI: 29.9–75.6]	34 [CI: 31.0–47.6]	0.43
Mean nodule hypervascularity	1.67 ± 0.46	1.53 ± 0.28	0.22	1.14 ± 0.25	1.41 ± 0.36	0.11
BCLC						
A	10/27 (37%)	19/26 (73.1%)	0.009	0	0	1
B	17/27 (73%)	7/26 (26.9%)		7/7 (100%)	24/24 (100%)	
Clinical indication						
Downstaging	4/27 (14.8%)	1/26 (3.8%)	0.37	0	0	1
Bridging	8/27 (29.6%)	10/26 (38.5%)		0	0	
Palliative	15/27 (55.6%)	15/26 (57.7%)		7/7 (100%)	24/24 (100%)	

balloon inflation following forced injection, visualization of vascular anastomosis that could determine potential non-target embolization, and manual perception of resistance to embolic injection). Immediately after reaching the respective endpoints, a Ne-CBCT was performed. On Ne-CBCT, all embolized nodules were completely segmented on a single slice in which the maximum lesion diameter (defined as ROI), the signal (pseudo-attenuation [HU*]), and the noise (SD) of the ROI were recorded. This operation was performed twice and then compared [16, 17]. In addition, three ROIs [TR] were taken in the non-embolized liver (area: 1 cm^2 each). The contrast was defined as the difference between the signal and the signal average of the surrounding non-embolized liver parenchyma. Ne-CBCT was evaluated by one radiologist (4 years of experience) blinded to the treatment allocation.

SIRT and b-SIRT

All procedures were performed by one experienced (> 15 years) interventional radiologist. In all cases, a treatment simulation by injection of technetium-99 m (99mTc) macro-aggregated albumin (MAA) was done from the appropriate feeder artery and evaluated by SPECT imaging [18]. The differences between SIRT and b-SIRT included a 2.7 Fr micro-catheter or a balloon micro-catheter both performed with resin-based microspheres. Post-therapy SPECT/CT (Symbia IntevoTM system; Siemens, Erlangen, Germany) scan was performed between 1 and 20 h after SIRT to evaluate the 90Y-microspheres distribution (SIR-spheres Y-90 resin-microspheres, Sirtex Medical Europe, Bonn, Germany). Post-therapy SPECT/CT imaging was used to perform 2D and 3D dosimetry as described below.

As a first step, the accuracy and intensity of 90Y-resin-microspheres activity distribution were evaluated by comparing the 2D activity intensity peak (Pixel Value) of the signal along a line crossing the treated area between patients treated with or without balloon micro-catheter. The higher the peak, the more intense was the signal inside the treated area.

Then, 3D effective dose in Gy was delivered to the target, and normal liver per unit cumulated activity (GBq) was calculated based on the activity distribution on SPECT/CT imaging. Lesion and normal liver were delineated on MIM 6.1.7 workstation (MIM Software Inc., Cleveland, Ohio), and dose calculation was performed on the obtained volumes [16, 19]. For each patient, the mean absorbed dose (< D >) in Gy obtained for normal liver and tumor were compared with expected values (< D > to tumor > 100 Gy, < D > to normal liver < 40 Gy). The SPECT/CT images were interpreted by one radiologist (4 years of experience) blinded to treatment allocation together with a medical physicist (5 years of experience).

Anatomopathological Analysis

Haematoxylin/eosin-stained histological sections of HCC nodules were examined microscopically, and the PEG microsphere presence was recorded in both peri-tumoral and intra-tumoral areas by counting the total number of PEG particles. The blinded pathologist examined all sections in which the tumor site of treatment was appreciable. Maximum interslice gap was 3 mm. The anatomopathological specimen was evaluated by a pathologist with 20 years of experience.

Study Outcomes

The aim of this study was to observe the different concentrations of PEG microspheres (TACE and anatomopathological specimen) and 90Y-microspheres (SIRT) in patients who underwent micro-balloon catheter versus standard trans-arterial therapies. Therefore, the evaluations were done at (1) post-TACE quantitative pseudo-attenuation analysis on Ne-CBCT, (2) post-SIRT SPECT dose analysis, and (3) PEG microspheres deposition in the anatomopathological specimen following OLT.

Assessment of treatment response was categorized according to mRECIST criteria [20] at 1 and 3 months after both treatments.

Statistical Analysis

Continuous variable group normality was tested using the Kolmogorov–Smirnov Z test. Continuous data were described as the mean value ± SD, whereas non-Gaussian with median and confidence interval 95%. T Student test or Mann–Whitney test was used according to data distribution. P-value < 0.05 was defined as statistical significance. Each P-value was calculated using a two-tailed significance level. Statistical analysis was performed using MedCalc 8.0 software (MedCalc Software bvba, Ostend, Belgium).

Results

All TACE treatments [53/84 (63.1%) patients] were performed in "Sapienza" hospital from January 2018 (first usage of balloon micro-catheter) to January 2019 divided into 26/53 (49.1%) DEB-TACE and 27/53 (50.9%) b-TACE. All SIRT treatments [31/84 (36.9%) patients] were performed in "Regina Elena" hospital from March 2018 (first usage of balloon micro-catheter) to January 2019, divided into 24/31 (77.4%) SIRT and 7/31 (22.6%) b-SIRT. From the total cohort of 84 patients: 5/53 (9.4%) patients of the TACE subgroup, 2/27 (7.4%) from the b-DEB-TACE subgroup, and 3/26 (11.5%) from the DEB-TACE subset underwent OLT. Radiological tumoral characteristics of all patients enrolled are summarized in Table 1.

Fifty-three patients were analyzed in the TACE group. Contrast, signal-to-noise ratio, and contrast-to-noise ratio were significantly higher in b-DEB-TACE vs. DEB-TACE subgroup (182.33 pseudo-HU [CI95% 160.3–273.5] vs. 124 pseudo-HU [CI95% 80.6–163.6]; 8.3 [CI95% 5.7–10.1] vs 0.4.5 [CI95% 3.7–6.0]; 6.9 [CI95% 4.3–7.8] vs. 3.1 [CI95% 2.2–5.0] $p < 0.05$, respectively). Figure 2 shows a comparison between a TACE and a b-DEB-TACE patient. B-DEB-TACE signal had a trend of superiority, without reaching statistical significance, compared with DEB-TACE nodules (229.0 [CI95% 206.2–337.5] vs. 195.5 [CI95% 117.5–240.5]; $p = 0.07$, respectively (Table 2).

Thirty-one patients were analyzed in the SIRT group. b-SIRT had a better dosimetry profile both in 2D and 3D analyses. Concerning 2D evaluation, the activity intensity peak was significantly higher in the b-SIRT subgroup than SIRT (987.5 ± 393.8 vs. 567.7 ± 302.2, $p = 0.005$), a higher quantity of Y90-microspheres was delivered to the target area of treatment with the same administered activity. In regard to the 3D dose analysis (expression of Absorbed Dose in Gy), the mean dose $< D >$ administered to the treated areas was significantly higher in the b-SIRT group than SIRT (151.6 Gy ± 53.2 vs. 100.1 Gy ± 43.4, $p = 0.01$) with almost no increase of the mean dose delivered to the normal liver (29.4 Gy ± 5.7 vs. 28.0 Gy ± 8.8, $p = 0.70$). Figure 3 compares SIRT and b-SIRT patients with similar anatomy, lesion size, and lesion location.

After the specimen analysis, a trend was noted for higher intra-tumoral localization of the PEG microspheres for b-DEB-TACE compared to DEB-TACE (72.9 particles/mm^2 ± 21.9 vs. 25.0 particles/mm^2 ± 22.9, $p = 0.10$) (Fig. 4).

Discussion

This study demonstrates the improved embolization performance obtained using a micro-balloon leading to higher microspheres concentration and higher therapeutic dose delivered to the lesions. The three adopted methodologies (Ne-CBCT, 2D and 3D analysis at SPECT/CT, and intratumor microspheres deposition observed during the pathological specimen analysis) converge to demonstrate an advantage of micro-balloon interventions regardless of the different embolic agent employed. These technical advantages could lead to several clinical benefits in different fields of application.

Regarding TACE, Ne-CBCT assessed the deposition of embolic material at the end of the embolization procedure [5, 21]. Ne-CBCT demonstrated the ability of temporary occlusion micro-balloon through higher contrast signal and contrast to noise ratio, thus permitting maximization of embolic agent uptake within the target lesion compared to the standard non-occluded procedure, sparing surrounding healthy liver parenchyma (Fig. 2). This evidence has several potential impacts on clinical practice: on one side, a higher dose of the administered drug to the target tumor correlates with the better procedural oncological outcome regardless of the sort of catheter employed [22]; on the

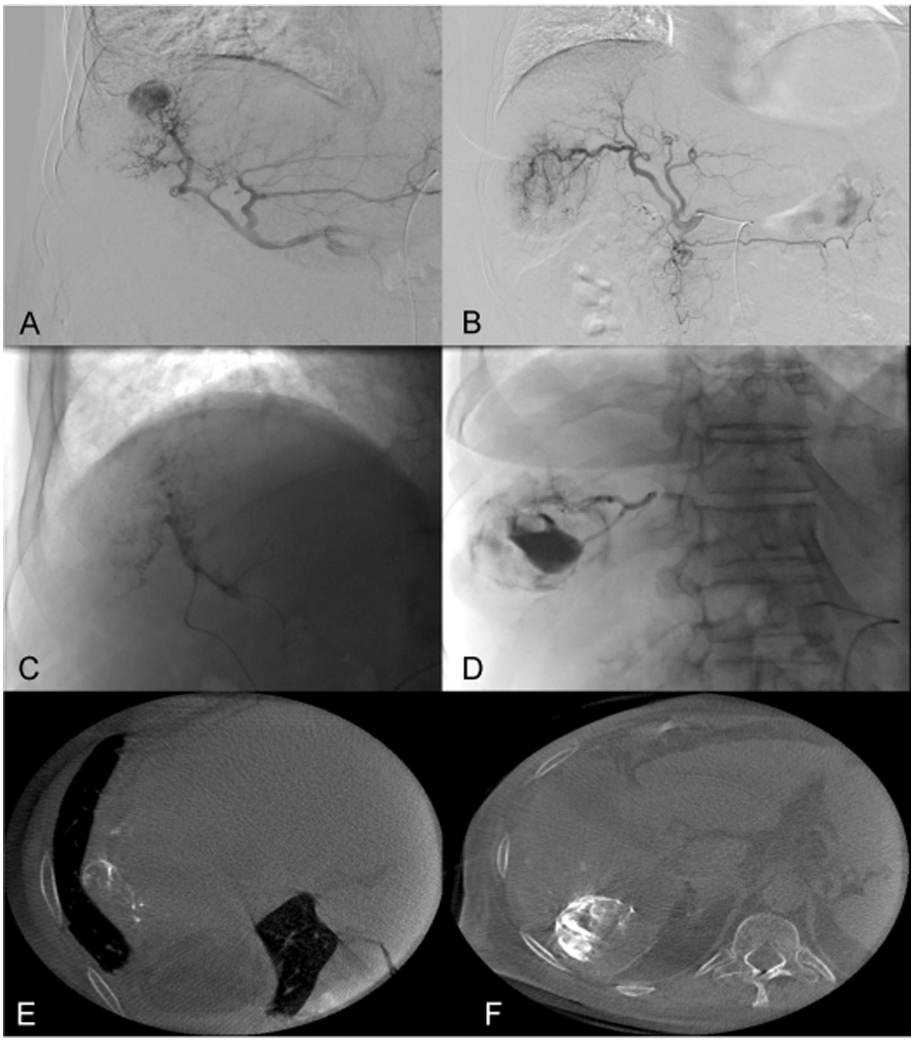

Fig. 2 A comparison between DEB-TACE (left column) and B-TACE (right column) clinical cases. **A–B**: pre-embolization right oblique digital subtraction angiography (DSA) demonstrate hypervascular HCC; **C–D**: single shot non subtracted x-ray acquired immediately after the end of the embolization demonstrate a partial contrast stain in the TACE procedure (**C**) and a high density on contrast at the end of b-TACE procedure (**D**). **E–F**: post-procedural not-enhanced cone-beam CT (Ne-CBCT) confirmed ad significantly different pseudo-attenuation of the nodule target of treatment

Table 2 CBCT parameters utilized in the study

Scan protocol	
External detector size and maximum FoV (cm)	30 × 40
Voxel size	0.3
Matrix size	1.920 × 2.480
Cone angle	220°
Rotational angle	200°
Rotation speed	60 f/s
Duration scan time	5 s

other hand, liver reserve sparing is a known significant factor influencing post-TACE prognosis [23]. Moreover, having TACE procedures a fixed drug threshold, b-TACE has the advantage to ameliorate drug tumoral penetration (ameliorate drug penetration since a trend towards a better intra-tumoral microsphere penetration was observed at specimen analysis) and this could further enhance treatment response (Fig. 4).

Regarding SIRT, SPECT/CT imaging allows for quantification of the absorbed dose (Gy) within the lesion and the normal liver that is a key information for the radiological effect assessment, and could allow to predict the treatment success and/or complications such as radioembolization-induced liver disease [24]. In this cohort, micro-balloon interventions allowed a more accurate dose distribution with the same amount of administered activity. A higher signal intensity, represented by a higher 2D peak, was assessed for the micro-balloon group. This data derives from the increment of the 90Y-microspheres uptake and deposition inside the lesion for b-SIRT compared to the standard SIRT procedure. Moreover, 3D dosimetry demonstrated that the balloon micro-catheter use leads to achieving a higher mean absorbed dose (> 150 Gy) in the lesion without increasing the dose delivered to surrounding liver parenchyma. This aspect could result in an improved efficacy and safety profile of the SIRT procedures, with a more steep and sharp dose curve, limiting injuries to the

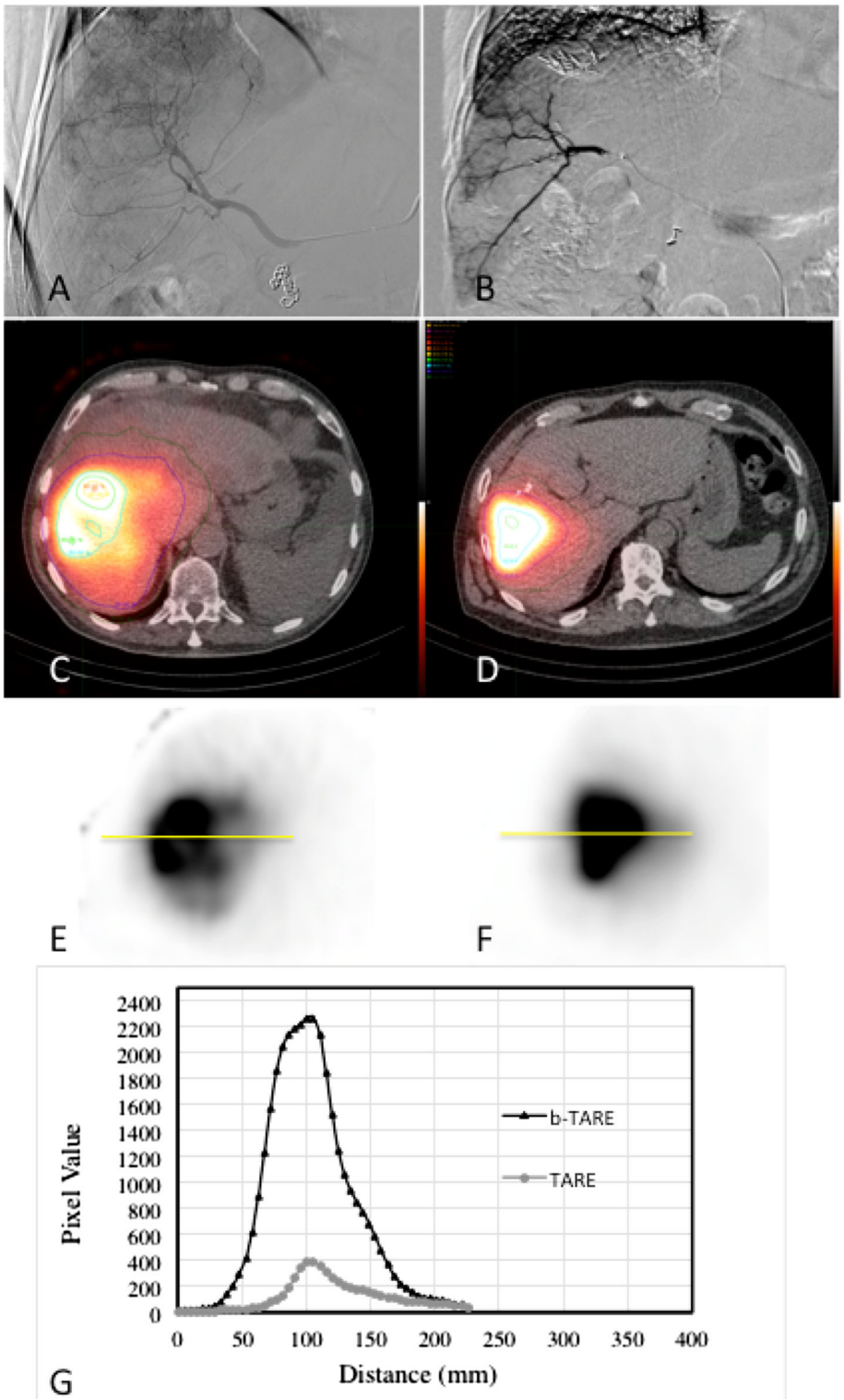

Fig. 3 A comparison between a SIRT (left column) and b-SIRT (right column) patient that had similar anatomy, lesion size, and lesion location. **A–B**: pre-embolization digital subtraction angiography (DSA); **C–D**: dose curves in Gy visualized on post-treatment Y90 SPECT/CT images; **E–G**: visualization and comparison of the 2D activity intensity peaks of the signal along a line crossing the lesion on SPECT images

surrounding parenchyma while higher therapeutic doses are delivered to the target tumor (Fig. 3).

The perception of a better efficacy profile with the use of the balloon micro-catheter lead the two centres to progressively increase in their clinical practice the dimension of nodules selected for this new technique, resulting in larger median diameters for the balloon micro-catheter cohort treated with TACE. The final composition

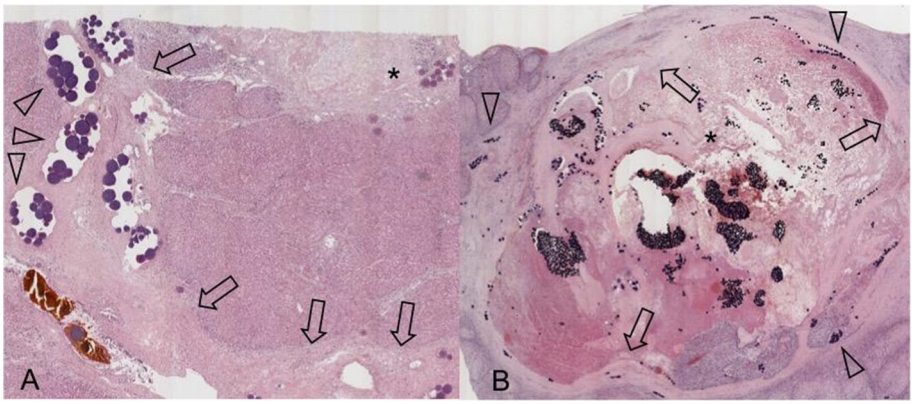

Fig. 4 Anatomopathological images showing hematoxylin–eosin-stained histological sections of HCC nodules after OLT. **A**: post-TACE OLT. PEG particles presence was recorded predominantly in peri-tumoral areas (arrowhead). **B**: post-b-TACE OLT. PEG particles presence was recorded predominantly in intra-tumoral areas. (asterisk). The black arrow depicts the tumor capsule

of cohorts reflects the hypothesis that the larger the tumor, the more benefit is obtained from this technique. This consideration led to a progressive increase of median target nodule diameter enrolled in both institutions, as depicted by the larger median diameter of the balloon occluded cohort (B-TACE; B-SIRT). However, a statistically significant difference in mean diameter was observed only for TACE treatments because TACE lesions are usually smaller in diameter if compared with SIRT.

No differences were found regarding contrast enhancement in pre-procedural CT between b-DEB-TACE versus DEB-TACE and b-SIRT versus SIRT (1.67 ± 0.46 vs 1.53 ± 0.28; 1.14 ± 0.25 vs. 1.41 ± 0.36; respectively; $p > 0.05$).

During the period in which treatments were conducted (January 2018–March 2019), no technical guidelines recommending which patients may benefit from balloon-occluded microcatheter-based procedures were published; thus, as mentioned above, the decision for employing balloon micro-catheter was at the discretion of the operator.

The main limitations of the study are its retrospective and not randomized nature. Only a few patients have a pathological correlation in the TACE arm, and no patient underwent liver transplantation in the SIRT group because of their baseline BCLC staging. These limitations are because data were derived from our Institutional datasets and they are representative of a wide variety of patients. Another limitation is that Ne-CBCT was evaluated by a single reader and last, pre-yttrium studies in the SIRT arm were not performed using a balloon microcatheter, potentially leading to different dosimetry.

The results of the present study demonstrate in vivo, due to the use of three different methods, the ameliorative embolization profile (measured as higher target lesion signal at Ne-CBCT post-b-TACE, a higher signal at SPECT/CT post-b-SIRT, and higher lesion absorbed dose post-b-SIRT) of oncological interventions performed with the balloon micro-catheter. These results are of relevance because they are coherent even if derived from two different clinical settings and the advantage is appreciable regardless of the embolic employed (drug-eluting beads for TACE or radioisotope for SIRT). This advantage could translate into improved performance of the oncological catheter-based treatments that will require to be validated in large-scale studies.

Acknowledgements None.

Declarations

Conflict of interest The authors declare that they have no conflict of interest.

References

1. Irie T, Kuramochi M, Takahashi N. Dense accumulation of lipiodol emulsion in hepatocellular carcinoma nodule during selective balloon-occluded transarterial chemoembolization: measurement of balloon-occluded arterial stump pressure. Cardiovasc Interv Radiol. 2013;36(3):706–13.
2. Aramburu J, Anton R, Rivas A, et al. Numerical zero-dimensional hepatic artery hemodynamics model for balloon-occluded transarterial chemoembolization. Int J Numer Method Biomed Eng. 2018;34(7):e2983.
3. Saltarelli A, Pelle G, Notarianni E, Pasqualini V, Cianni R. Y90 radioembolization with Occlusafe catheter infusion system in patients with unresectable hepatic metastasis. J Vasc Interv Radiol. 2017;28(2):S213–4.
4. Golfieri R, Bezzi M, Verset G, et al. Retrospective European multicentric evaluation of selective transarterial chemoembolisation with and without balloon-occlusion in patients with hepatocellular carcinoma: a propensity score matched analysis. Cardiovasc Interv Radiol. 2021;44(7):1048–59.
5. Lucatelli P, De Rubeis G, Basilico F, et al. Sequential dual-phase cone-beam CT is able to intra-procedurally predict the one-month treatment outcome of multi-focal HCC, in course of degradable starch microsphere TACE. Radiol Med (Torino). 2019;124(12):1212–9.
6. Lucatelli P, Argirò R, De Rubeis G, et al. Polyethylene glycol epirubicin-loaded transcatheter arterial chemoembolization procedures utilizing a combined approach with 100 and 200 μm Microspheres: a promising alternative to current standards. J Vasc Interv Radiol. 2019;30(3):305–13.

7. Lucatelli P. Polyethylene glycol (PEG)-Epirubicin loaded drug-elunting embolic (DEE)-TACE procedures utilizing a combined approach with 100- and 200- μm microspheres: iniatial experience. J Vasc Interv Radiol. 2018;30(3):305–13.
8. Park HJ, Kim JH, Choi S-y, et al. Prediction of therapeutic response of hepatocellular carcinoma to transcatheter arterial chemoembolization based on pretherapeutic dynamic CT and textural findings. Am J Roentgenol. 2017;209(4):W211–20.
9. O'Donohoe RL, Kavanagh RG, Cahalane AM, Houlihan DD, McCann JW, Ryan ER. C-arm cone-beam CT parenchymal blood volume imaging for transarterial chemoembolization of hepatocellular carcinoma: implications for treatment planning and response. Eur Radiol Exp. 2019;3(1):21.
10. Goedicke A, Berker Y, Verburg FA, Behrendt FF, Winz O, Mottaghy FM. Study-parameter impact in quantitative 90-Yttrium PET imaging for radioembolization treatment monitoring and dosimetry. IEEE Trans Med Imaging. 2013;32(3):485–92.
11. Auditore L, Amato E, Italiano A, Arce P, Campennì A, Baldari S. Internal dosimetry for TARE therapies by means of GAMOS Monte Carlo simulations. Phys Med: PM: Int J Devot Appl Phys Med Biol: Off J Italian Assoc Biomed Phys (AIFB). 2019;64:245–51.
12. Lucatelli P, De Rubeis G, GinnaniCorradini L, et al. Intra-procedural dual phase cone beam computed tomography has a better diagnostic accuracy over pre-procedural MRI and MDCT in detection and characterization of HCC in cirrhotic patients undergoing TACE procedure. Eur J Radiol. 2020;124:108806.
13. Chernyak V, Fowler KJ, Kamaya A, et al. Liver imaging reporting and data system (LI-RADS) version 2018: imaging of hepatocellular carcinoma in at-risk patients. Radiology. 2018;289(3):816–30.
14. Mitchell DG, Bruix J, Sherman M, Sirlin CB. LI-RADS (liver imaging reporting and data system): summary, discussion, and consensus of the LI-RADS management working group and future directions. Hepatology. 2015;61(3):1056–65.
15. Choi JY, Lee JM, Sirlin CB. CT and MR imaging diagnosis and staging of hepatocellular carcinoma: part I. Development, growth, and spread: key pathologic and imaging aspects. Radiology. 2014;272(3):635–54.
16. Sagara Y, Hara AK, Pavlicek W, Silva AC, Paden RG, Wu Q. Abdominal CT: comparison of low-dose CT with adaptive statistical iterative reconstruction and routine-dose CT with filtered back projection in 53 patients. Am J Roentgenol. 2010;195(3):713–9.
17. Goenka AH, Herts BR, Dong F, et al. Image noise, CNR, and detectability of low-contrast, low-attenuation liver lesions in a Phantom: effects of radiation exposure, phantom size, integrated circuit detector, and iterative reconstruction. Radiology. 2016;280(2):475–82.
18. Padia SA, Lewandowski RJ, Johnson GE, et al. Radioembolization of hepatic malignancies: background, quality improvement guidelines, and future directions. J Vascu Interv Radiol: JVIR. 2017;28(1):1–15.
19. Dewaraja YK, Frey EC, Sgouros G, et al. MIRD pamphlet No. 23: quantitative SPECT for patient-specific 3-dimensional dosimetry in internal radionuclide therapy. J Nucl Med Off Pub Soc Nuc Med. 2012;53(8):1310–25.
20. Lencioni R, Llovet JM. Modified RECIST (mRECIST) assessment for hepatocellular carcinoma. Semin Liver Dis. 2010;30(1):52–60.
21. Lucatelli P, Argiro R, Bascetta S, et al. Single injection dual phase CBCT technique ameliorates results of trans-arterial chemoembolization for hepatocellular cancer. Trans Gastroenterol Hepatol. 2017;2:83.
22. Lu W, Li YH, He XF, Zhao JB, Chen Y, Mei QL. Necrosis and apoptosis in hepatocellular carcinoma following low-dose versus high-dose preoperative chemoembolization. Cardiovasc Interv Radiol. 2008;31(6):1133–40.
23. Ho SY, Liu PH, Hsu CY, et al. Prognostic role of noninvasive liver reserve markers in patients with hepatocellular carcinoma undergoing transarterial chemoembolization. PloS one. 2017;12(7):e0180408.
24. Alsultan AA, Smits MLJ, Barentsz MW, Braat AJAT, Lam MGEH. The value of yttrium-90 PET/CT after hepatic radioembolization: a pictorial essay. Clin Trans Imaging. 2019;7(4):303–12.